

Centralized Cooperative Spectrum Sensing from Sub-Nyquist Samples for Cognitive Radios

Deborah Cohen, Alon Akiva, Barak Avraham, Yonina C. Eldar
Technion - Israel Institute of Technology, Haifa, Israel
{debby@tx, sakalon2@t2, sbarakav@t2, yonina@ee}.technion.ac.il

Abstract—Cognitive Radio (CR) challenges the traditional task of spectrum sensing with requirements of reliability, efficiency and real-time. Sub-Nyquist sampling has been considered for this task in order to cope with the sampling rate bottleneck of the wideband signals a CR usually deals with, by exploiting their multiband structure. However, communication signals suffer from fading and shadowing effects that affect a single CR's performance. In this paper, we consider collaborative spectrum sensing by a network of CRs, each sharing an observation matrix derived from sub-Nyquist samples of their respective received signal with a fusion center. Exploiting the fact that all received signals share a joint support, equal to that of the transmitted signal, the fusion center recovers it by combining the measurements of the different CRs. We present two joint reconstruction algorithms, Block Sparse Simultaneous Orthogonal Matching Pursuit (BSOMP) and Block Sparse Simultaneous Iterative Hard Thresholding (BSIHT), that adapt the original OMP and IHT to both block sparse and matrix (simultaneous) inputs. Simulations show that our algorithms outperform a collaborative scheme based on hard decisions, namely the union of the supports recovered by each CR individually, demonstrating that cooperation between CRs via measurement fusion improve their performance.

I. INTRODUCTION

Cognitive Radio (CR), introduced by Mitola [1], has been recently considered as a promising solution to the ever-increasing spectrum crowdedness [2], [3]. Secondary users would opportunistically access frequency bands left vacant by their primary owners, called white space or spectrum holes, increasing spectral efficiency. Spectrum sensing is an essential task in the CR's cycle [3]. Indeed, a CR should be able to constantly monitor the spectrum and detect the primary users' (PUs) activity, reliably and fast [4], [5]. Besides, in order to increase the chance to find an unoccupied spectral band, the CR has to sense a wide band of spectrum. Nyquist rates of wideband signals are high and can even exceed today's best analog-to-digital converters (ADCs) front-end bandwidths. Moreover, such high sampling rates generate a large number of samples to process, affecting speed and power consumption.

To overcome the rate bottleneck, several new sampling methods have recently been proposed [6], [7] that reduce the sampling rate in multiband settings below the Nyquist rate. The authors consider perfect signal reconstruction in noise-free settings and provide sampling and recovery techniques. In the CR setting, however, only the signal support is of interest and reconstructing the original signal is unnecessary. Several

papers have considered power spectrum, rather than spectrum reconstruction, from sub-Nyquist samples [8], [9], [10].

The task of spectrum sensing for CRs is further complicated due to path loss, fading and shadowing [11], [12]. To overcome these practical issues, collaborative CR networks have been considered, where different users share their sensing results and cooperatively decide on the licensed spectrum occupancy. Cooperative spectrum sensing can be classified into three categories based on the way the data is shared by the CRs in the network: centralized, distributed and relay-assisted. Moreover, two options of data fusion arise: decision fusion, or hard decision, where the CRs only report their binary local decisions, and measurement fusion, or soft decision, where they share all or part of their samples [11]. In [13], the authors compare soft and hard decisions using sequential detection. They consider the Nyquist samples of one spectral band. Cooperation has been shown to improve the detection performance and relax sensitivity requirements by exploiting spatial diversity [12], [14]. The authors [12], [14] quantify the effect of collaboration on the probabilities of detection and false alarm in the Nyquist regime and in centralized settings. In [12], an OR-rule based on the binary decisions of the sensors is used as a fusion rule, whereas a joint optimization problem is solved in [14] to find the optimal decision threshold.

In this paper, we focus on centralized cooperation based on measurement fusion, which requires a fusion center. Several works have considered centralized collaborative wideband spectrum sensing for cognitive radios. In [15], each CR, equipped with a frequency selective filter, senses a linear combination of multiple predefined narrow frequency bands. Each band is represented by a binary state, 1 or 0, indicating if it is occupied or not, rather than an actual signal. The support of the wideband signal is then recovered at the fusion center from the samples sent by the CRs, using matrix completion and joint sparsity recovery techniques. However, this technique requires additive analog filters at each CR. Moreover, since the CRs do not sense the whole spectrum, a large part of spatial diversity is not exploited. Furthermore, no actual signals are considered and no sampling and acquisition method is described. A centralized approach, where all samples from the CRs are sent to a fusion center, is proposed in [16]. Here, each CR samples the wideband signal, assumed to be sparse, at a sub-Nyquist rate. However, in order to derive their reconstruction scheme, the authors exploit a relation between sub-Nyquist and Nyquist samples, whereas no specific sampling scheme is given. Moreover, the channel state information (CSI) is assumed to be known. Both non fading and fading environments are considered but no analysis on the reconstruction is provided for the latter. In [17], no concrete sampling scheme is given as well, and the sampling matrix

This work is supported in part by the Semiconductor Research Corporation (SRC) through the Texas Analog Center of Excellence (TxACE) at the University of Texas at Dallas (Task ID:1836.114), in part by the Israel Science Foundation under Grant no. 170/10, in part by the Ollendorf foundation, and in part by the Intel Collaborative Research Institute for Computational Intelligence (ICRI-CI). Deborah Cohen is grateful to the Azrieli Foundation for the award of an Azrieli Fellowship.

is assumed to be random Gaussian. The signal of interest, represented by a finite discrete sequence and assumed to be sparse, is jointly recovered at a fusion center from the measurements of the different CRs. A distributed approach is considered in [18] that is first exposed in a centralized manner. The goal of that work is to estimate the power distribution in space and frequency. The authors use a discretized grid both in space and frequency and do not recover the emitted signal continuous support.

In this work, we propose a centralized collaborative spectrum sensing method from samples acquired at a sub-Nyquist rate at each CR. We use either multicoset sampling [6] or the Modulated Wideband Converter (MWC) [7] for the sampling stage. The CRs sample the wideband sparse signal suffering from different effects of fading and shadowing, and share an observation matrix derived from their low-rate samples, rather than the samples themselves to reduce communication overhead, with a fusion center which recover the underlying joint support. The overhead in delay and energy caused by cooperative sensing, is mitigated by processing sub-Nyquist samples. We derive two reconstruction algorithms, Block Sparse Simultaneous Orthogonal Matching Pursuit (BSOMP) and Block Sparse Simultaneous Iterative Hard Thresholding (BSIHT), that adapt the Distributed Compressed Sensing Simultaneous OMP (DCS-SOMP) [19] and Simultaneous IHT (S-IHT) algorithms [17] to our settings. We do not assume any *a priori* knowledge on the CSI. We observe that both BSOMP and BSIHT outperform support recovery based on the union between the supports recovered by each CR independently.

This paper is organized as follows. In Section II, we present the transmitted and received signal models. Sections III and IV describe the individual sub-Nyquist sampling stage and joint support recovery stage, respectively. Numerical experiments are presented in Section V.

II. SIGNAL MODEL AND PROBLEM FORMULATION

A. Transmitted Signal Multiband Model

Let $x(t)$ be a real-valued continuous-time signal, supported on $\mathcal{F} = [-1/2T_{\text{Nyq}}, +1/2T_{\text{Nyq}}]$ and composed of up to N_{sig} transmissions, such that

$$x(t) = \sum_{i=1}^{N_{\text{sig}}} s_i(t), \quad (1)$$

where $s_i(t)$ is a bandpass process. The single-sided bandwidth of each transmission is assumed to not exceed B . Formally, the Fourier transform of $x(t)$ defined by

$$X(f) = \int_{-\infty}^{\infty} x(t)e^{-j2\pi ft} dt \quad (2)$$

is zero for every $f \notin \mathcal{F}$. We denote by $f_{\text{Nyq}} = 1/T_{\text{Nyq}}$ the Nyquist rate of $x(t)$. Only N_{sig} and B , or at least an upper bound for each, are assumed to be known. Denote by S the frequency support of $x(t)$ and $\kappa = 2N_{\text{sig}}$ its sparsity (the factor 2 stems from the fact that each signal contributes two symmetric frequency bands). The carrier frequencies and modulations of $s_i(t)$ are unknown. The signal is received by N_{rec} receivers.

B. Faded Received Signal

We consider two effects of the transmission channels: Rayleigh fading, or small-scale fading, and log-normal shadowing, or large-scale fading [20], [12], [21]. Denote by $r_{ij}(t)$ the received signal corresponding to the i th transmission, $1 \leq i \leq N_{\text{sig}}$, received at the j th CR, $1 \leq j \leq N_{\text{rec}}$. The received signal is generally described in terms of the transmitted signal $s_i(t)$ convolved with the impulse response of the channel $h_{ij}(t)$, namely

$$r_{ij}(t) = s_i(t) * h_{ij}(t), \quad (3)$$

where $*$ denotes convolution.

1) *Rayleigh fading*: For most practical channels, the free-space propagation model, which only accounts for path loss, is inadequate to describe the channel. A signal can travel from transmitter to receiver over multiple reflective paths, which is traditionally modeled as Rayleigh fading, namely the envelope of the channel responses $h_{ij}(t)$ follows the Rayleigh distribution, given by

$$p_h(r) = \begin{cases} \frac{r}{\sigma^2} e^{-r^2/2\sigma^2} & r \geq 0 \\ 0 & \text{otherwise,} \end{cases} \quad (4)$$

where r is the envelope amplitude of the received signal, and $2\sigma^2$ its mean power [21].

2) *Log-normal shadowing*: Large-scale fading represents the average signal power attenuation or path loss due to motion over large areas. This phenomenon is affected by prominent terrain contours between the transmitter and receiver. Empirical measurements suggest that this type of fading, or shadowing, follows a normal distribution in dB units [22], or alternatively, the linear channel gain may be modeled as a log-normal random variable [12]. Therefore, the path loss (PL) measured in dB is expressed as

$$PL = PL_0 + 10\gamma \log \frac{d}{d_0} + X_\sigma. \quad (5)$$

Here, the reference distance d_0 corresponds to a point located in the far field of the antenna (typically 1 km for large cells). The path loss to the reference point PL_0 is usually found through field measurements or calculated using free-space path loss. The value of the path loss exponent γ depends on the frequency, antenna heights, and propagation environment. Finally, X_σ denotes a Gaussian random variable (in dB) with variance σ^2 determined heuristically as well [21].

The shadowed received signal is thus given by

$$r_{ij}(t) = 10^{-PL_{ij}/20} \cdot s_i(t), \quad (6)$$

where PL_{ij} denotes the path loss between the i th transmitter and the j th receiver. Here, $h_{ij}(t) = 10^{-PL_{ij}/20}$ is a constant.

C. Problem Formulation

A network of N_{rec} CRs receives the N_{sig} transmissions, such that the received signal at the j th CR is given by

$$x^{(j)}(t) = \sum_{i=1}^{N_{\text{sig}}} r_{ij}(t). \quad (7)$$

Our goal is to assess the support of the transmitted signal $x(t)$ from sub-Nyquist samples of the received $x^{(j)}(t)$, $1 \leq j \leq N_{\text{rec}}$.

The transmissions are affected differently by fading and shadowing effects from each transmitter to each CR. In order to determine the support of $x(t)$, we exploit the joint sparsity in the frequency domain shared by $x^{(j)}(t)$, $1 \leq j \leq N_{\text{rec}}$. Specifically, we jointly recover the common support of $x^{(j)}(t)$ from their sub-Nyquist samples, which is the support of the original signal $x(t)$ as well, namely S .

III. INDIVIDUAL SUB-NYQUIST SAMPLING

In this section, we briefly describe the sub-Nyquist sampling schemes performed at each CR on the corresponding received signal $x^{(j)}(t)$. We consider two different approaches: multicoset sampling [7] and the MWC [6] which were previously proposed for sparse multiband signals. We show that both schemes lead to identical expressions of the signal spectrum in terms of the samples. Therefore, the support reconstruction stage presented in Section IV can be applied to either of the samples. For convenience, we drop the index j in this section.

A. Multicoset sampling

Multicoset sampling [23] can be described as the selection of certain samples from the uniform grid. More precisely, the uniform grid is divided into blocks of N consecutive samples, from which only M are kept. The i th sampling sequence is defined as

$$x_{c_i}[n] = \begin{cases} x(nT_{\text{Nyq}}), & n = mN + c_i, m \in \mathbb{Z} \\ 0, & \text{otherwise,} \end{cases} \quad (8)$$

where $0 < c_1 < c_2 < \dots < c_M < N-1$. Let $f_s = \frac{1}{NT_{\text{Nyq}}} \geq B$ be the sampling rate of each channel and $\mathcal{F}_s = [-f_s/2, f_s/2]$. Following the derivations from multicoset sampling [7], we obtain

$$\mathbf{z}(f) = \mathbf{A}\mathbf{x}(f), \quad f \in \mathcal{F}_s, \quad (9)$$

where $\mathbf{z}_i(f) = X_{c_i}(e^{j2\pi f T_{\text{Nyq}}})$, $0 \leq i \leq M-1$ are the discrete-time Fourier transforms (DTFTs) of the multicoset samples and

$$\mathbf{x}_k(f) = X(f + K_k f_s), \quad 1 \leq k \leq N, \quad (10)$$

where $K_k = k - \frac{N+1}{2}$, $1 \leq k \leq N$ for odd N and $K_k = k - \frac{N+2}{2}$, $1 \leq k \leq N$ for even N . Each entry of $\mathbf{x}(f)$ is referred to as a bin since it consists of a slice of the spectrum of $x(t)$. The ik th element of the $M \times N$ matrix \mathbf{A} is given by

$$\mathbf{A}_{ik} = \frac{1}{NT_{\text{Nyq}}} e^{j\frac{2\pi}{N} c_i K_k}. \quad (11)$$

B. MWC sampling

The MWC [6] is composed of M parallel channels. In each channel, an analog mixing front-end, where $x(t)$ is multiplied by a mixing function $p_i(t)$, aliases the spectrum, such that each band appears in baseband. The mixing functions $p_i(t)$ are required to be periodic with period T_p such that $f_p = 1/T_p \geq B$. The function $p_i(t)$ has a Fourier expansion

$$p_i(t) = \sum_{l=-\infty}^{\infty} c_{il} e^{j\frac{2\pi}{T_p} lt}. \quad (12)$$

In each channel, the signal goes through a lowpass filter with cut-off frequency $f_s/2$ and is sampled at the rate $f_s \geq f_p$. For the sake of simplicity, we choose $f_s = f_p$. Repeating the calculations in [6], we derive the relation between the known DTFTs of the samples $y_i[n]$ and the unknown $X(f)$

$$\mathbf{z}(f) = \mathbf{A}\mathbf{x}(f), \quad f \in \mathcal{F}_s, \quad (13)$$

where $\mathbf{z}(f)$ is a vector of length N with i th element $z_i(f) = Y_i(e^{j2\pi f T_s})$. The unknown vector $\mathbf{x}(f)$ is given by (10). The $M \times N$ matrix \mathbf{A} contains the coefficients c_{il} :

$$\mathbf{A}_{il} = c_{i,-l} = c_{il}^*. \quad (14)$$

For both sampling schemes, the overall sampling rate is

$$f_{\text{tot}} = Mf_s = \frac{M}{N} f_{\text{Nyq}}. \quad (15)$$

C. Continuous to Finite (CTF)

The sets of equations (9) and (13) consist of an infinite number of linear systems since f is a continuous variable. Such systems are known as infinite measurement vectors (IMV) in the compressed sensing (CS) literature. We use the support recovery paradigm from [7] that produces a finite system of equations, called multiple measurement vectors (MMV) from an infinite number of linear systems. This reduction is performed by what is referred to as the continuous to finite (CTF) block.

From (9) or (13), we have

$$\mathbf{Q} = \mathbf{A}\mathbf{Z}\mathbf{A}^H \quad (16)$$

where

$$\mathbf{Q} = \int_{f \in \mathcal{F}_s} \mathbf{z}(f)\mathbf{z}^H(f)df \quad (17)$$

is a $M \times M$ matrix and

$$\mathbf{Z} = \int_{f \in \mathcal{F}_s} \mathbf{x}(f)\mathbf{x}^H(f)df \quad (18)$$

is a $N \times N$ matrix. We then construct a frame \mathbf{V} such that $\mathbf{Q} = \mathbf{V}\mathbf{V}^H$. Clearly, there are many possible ways to select \mathbf{V} . We construct it by performing an eigendecomposition of \mathbf{Q} and choosing \mathbf{V} as the matrix of eigenvectors corresponding to the non zero eigenvalues. We can then define the following linear system

$$\mathbf{V} = \mathbf{A}\mathbf{U}. \quad (19)$$

From [7] (Propositions 2-3), the support of the unique sparsest solution of (19) is the same as the support of the original set of equations (9) or (13).

IV. JOINT SUPPORT RECONSTRUCTION

In this section, we consider joint support recovery from the observation matrices $\mathbf{V}^{(j)}$, $1 \leq j \leq N_{\text{rec}}$ shared by the CRs with the fusion center and develop two joint support recovery algorithms: BSOMP and BSIHT.

A. Simultaneous Block Sparsity

The j th CR shares its observation matrix $\mathbf{V}^{(j)}$ and its measurement matrix $\mathbf{A}^{(j)}$ with the fusion center. The sampling matrices are considered to be different from one another in order to allow for more measurement diversity. However, the same known matrix can be used to reduce the communication overhead. The underlying matrices $\mathbf{U}^{(j)}$ are jointly sparse since fading (3, 4) and shadowing (6) do not affect the original signal support.

In the next section, we show how the joint support of $\mathbf{U}^{(j)}$, $1 \leq j \leq N_{\text{rec}}$, namely S , can be recovered from the measurements $\mathbf{V}^{(j)}$, $1 \leq j \leq N_{\text{rec}}$. We note that the matrices $\mathbf{V}^{(j)}$ are of size $M \times P$, where $P = \text{rank}(\mathbf{Q}) \leq M$.

We begin by expressing the set of equations (19), for $1 \leq j \leq N_{\text{rec}}$, in block sparse structure. Note that manipulating large block matrices, considered here for simplicity, is not needed and the computation is done on the different blocks separately, as is shown below. Denote the block observation matrix, which stacks the observation matrices vertically,

$$\mathbf{V} = \begin{bmatrix} \mathbf{V}^{(1)} \\ \mathbf{V}^{(2)} \\ \vdots \\ \mathbf{V}^{(N_{\text{rec}})} \end{bmatrix}, \quad (20)$$

the block measurement matrix

$$\mathbf{A} = \begin{bmatrix} \mathbf{A}_1^{(1)} & \dots & 0 & \dots & \mathbf{A}_N^{(1)} & \dots & 0 \\ \vdots & \ddots & \vdots & \dots & \vdots & \ddots & \vdots \\ 0 & \dots & \mathbf{A}_1^{(N_{\text{rec}})} & \dots & 0 & \dots & \mathbf{A}_N^{(N_{\text{rec}})} \end{bmatrix}, \quad (21)$$

and the block sparse matrix of interest, which stacks the rows of the matrices $\mathbf{U}^{(j)}$ by aggregating the rows with identical indices,

$$\mathbf{U} = \begin{bmatrix} \mathbf{U}_1^{(1)T} \\ \vdots \\ \mathbf{U}_1^{(N_{\text{rec}})T} \\ \vdots \\ \mathbf{U}_N^{(1)T} \\ \vdots \\ \mathbf{U}_N^{(N_{\text{rec}})T} \end{bmatrix}. \quad (22)$$

Here $\mathbf{A}_i^{(j)}$ denotes the i th column of the matrix $\mathbf{A}^{(j)}$, corresponding to the j th receiver, and $\mathbf{U}_i^{(j)T}$ denotes the i th row of the matrix $\mathbf{U}^{(j)}$. The k th block of \mathbf{U} is denoted by

$$\mathbf{U}[k] = \begin{bmatrix} \mathbf{U}_k^{(1)T} \\ \vdots \\ \mathbf{U}_k^{(N_{\text{rec}})T} \end{bmatrix}, \quad (23)$$

and the corresponding k th block of \mathbf{A} is

$$\mathbf{A}[k] = \begin{bmatrix} \mathbf{A}_k^{(1)} & 0 & \dots & 0 \\ 0 & \mathbf{A}_k^{(2)} & \dots & 0 \\ \vdots & \vdots & \ddots & \vdots \\ 0 & \dots & 0 & \mathbf{A}_k^{(N_{\text{rec}})} \end{bmatrix}. \quad (24)$$

Obviously, $\mathbf{V}^{(j)} = \mathbf{A}^{(j)}\mathbf{U}^{(j)}$, $\forall 1 \leq j \leq N_{\text{rec}}$, if and only if $\mathbf{V} = \mathbf{A}\mathbf{U}$.

In order to find the joint support S , we exploit both the joint or simultaneous sparsity between the columns of \mathbf{U} and the block sparsity of \mathbf{U} . In the worst case, we require $M \geq 2\kappa$, leading to a minimal sampling rate of $2\kappa B$ for each CR [7].

B. BSOMP

To adapt the original OMP algorithm to our setting, we need to extend it to both the simultaneous and block sparse settings. We use the DCS-SOMP algorithm of [19], which extends the original SOMP [24] to allow for a different sampling matrix $\mathbf{A}^{(j)}$ for each receiver, increasing measurement diversity. In each iteration, the block index $n \in \{1, 2, \dots, N\}$ that accounts for the greatest amount of residual energy, namely the index of the measurement matrix column that holds the highest correlation with the residual matrix, across all receivers, is retained. To extend DCS-SOMP to the block sparse case, this index is selected as the one which maximizes the Frobenius norm of the block matrices $\mathbf{B}[n]$ (line 4 in Algorithm 1) corresponding to the residual projections over all the receivers (lines 6-7 in Algorithm 1). Thus, at each iteration, the block that is best matched to the residual \mathbf{R} is chosen, as in [25].

The resulting BSOMP iterations are described in Algorithm 1. Here, $\mathbf{B}_j^T[n]$ denotes the j th row of $\mathbf{B}[n]$, $\hat{\mathbf{U}}_{|S}$ and $\hat{\mathbf{U}}_{|S^c}$ are the estimated matrix \mathbf{U} reduced to its support set and the complement set of the latter, respectively. The notations \dagger , H , and $\|\cdot\|_F$ represent the Moore-Penrose pseudo-inverse, Hermitian operation and Frobenius norm, respectively.

As for the original OMP, several halting criteria can be considered. When the original joint sparsity is known, a sparsity-based criterion can be used, namely $|S| \leq \kappa$. Otherwise, a residual-based criterion, such as $\|\mathbf{R}\|_2 < \epsilon$, where ϵ is a selected threshold, is needed.

Algorithm 1 BSOMP

Input: observation matrices $\mathbf{V}^{(j)}$, measurement matrix $\mathbf{A}^{(j)}$

Output: index set S containing the joint support of $\mathbf{U}^{(j)}$

- 1: Initialization: residual $\mathbf{R} = \mathbf{V}$, index set $S = \emptyset$, $i = 0$
 - 2: **while** halting criterion false **do**
 - 3: $i \leftarrow i + 1$
 - 4: $\mathbf{B}_j^T[n] = (\mathbf{A}_n^{(j)})^H \mathbf{R}^{(j)}$, $j \in \{1, \dots, N_{\text{rec}}\}$
 - 5: **for** $n = 1$ to N **do**
 - 6: $b(n) = \|\mathbf{B}[n]\|_F^2$
 - 7: **end for**
 - 8: $S \leftarrow S \cup \arg \max_n b(n)$
 - 9: $\hat{\mathbf{U}}_{|S}^{(j)} \leftarrow (\mathbf{A}^{(j)})_{|S}^\dagger \mathbf{V}^{(j)}$, $\hat{\mathbf{U}}_{|S^c}^{(j)} \leftarrow 0$, $j \in \{1, \dots, N_{\text{rec}}\}$
 - 10: $\mathbf{R} \leftarrow \mathbf{V} - \sum_{k \in S} \mathbf{A}[k] \hat{\mathbf{U}}[k]$
 - 11: **end while**
 - 12: return S
-

C. BSIHT

Next, we turn to the BSIHT algorithm, which extends SIHT [17] to the block sparse case. SIHT solves problems of the type of (19) (for one receiver) by computing the estimate of columns of the sparse matrix, following the original IHT. The indices of the common support are then selected by averaging over these estimates [17]. In the collaborative problem, the average over the estimates is carried out over the columns of the sparse matrix as well as across the different receivers (lines 6-7 in Algorithm 2). Once the support is selected, the updated calculations are performed separately for each column of the sparse matrix and for each receiver. An adaptive step size is used to improve the performance with regard to a fixed scaling factor [17].

The resulting BSIHT is shown in Algorithm 2. Here, $\mathbf{U}_k^{(j)i}$ denotes the k th column of the matrix $\mathbf{U}^{(j)}$ estimated at the i th iteration, $\mathbf{Z}_k^{(j)}$ and $\mathbf{Z}_n^{T(j)}$ denote the k th column and n th row of the matrix $\mathbf{Z}^{(j)}$, respectively, H_{S^i} is a nonlinear operator that sets all but the indices of S^i to zero and $\mathcal{T}(\mathbf{b}, \kappa)$ selects the indices of the κ largest elements of \mathbf{b} .

Again, several halting criteria can be considered. A norm convergence criterion, which sums over all columns and all receivers, can be chosen. A maximum number of iterations can also be selected.

Algorithm 2 BSIHT

Input: observation matrices $\mathbf{V}^{(j)}$, measurement matrix $\mathbf{A}^{(j)}$

Output: index set S containing the joint support of $\mathbf{U}^{(j)}$

- 1: Initialization: $\mathbf{U}_k^{(j)0} = 0$, step size $\mu_k^{(j)0} = \frac{1}{M}$, $k \in \{1, \dots, P\}, j \in \{1, \dots, N_{\text{rec}}\}, i = 0$
 - 2: **while** halting criterion false **do**
 - 3: $\mathbf{Z}_k^{(j)i+1} = \mathbf{U}_k^{(j)i} + \mu_k^{(j)i} (\mathbf{A}^{(j)})^H (\mathbf{V}_k^{(j)} - \mathbf{A}^{(j)} \mathbf{U}_k^{(j)i})$,
 $k \in \{1, \dots, P\}, j \in \{1, \dots, N_{\text{rec}}\}$
 - 4: **for** $n = 1$ to N **do**
 - 5: Denote $\mathbf{B}_j^T[n] = \mathbf{Z}_n^{T(j)i+1}$, $k \in \{1, \dots, P\}, j \in \{1, \dots, N_{\text{rec}}\}$
 - 6: $b(n) = \|\mathbf{B}[n]\|_F^2$
 - end for**
 - 7: $S^i \leftarrow \text{supp}(\mathcal{T}(\mathbf{b}, \kappa))$
 - 8: $\mathbf{U}_k^{(j)i+1} = H_{S^i}(\mathbf{U}_k^{(j)i} + \mu_k^{(j)i} (\mathbf{A}^{(j)})^H (\mathbf{V}_k^{(j)} - \mathbf{A}^{(j)} \mathbf{U}_k^{(j)i}))$, $k \in \{1, \dots, P\}, j \in \{1, \dots, N_{\text{rec}}\}$
 - 9: $\mathbf{g}_k^{(j)i+1} = (\mathbf{A}^{(j)})^H (\mathbf{V}_k^{(j)} - \mathbf{A}^{(j)} \mathbf{U}_k^{(j)i+1})$, $k \in \{1, \dots, P\}, j \in \{1, \dots, N_{\text{rec}}\}$
 - 10: $\mu_k^{(j)i+1} = \frac{\|\mathbf{g}_k^{(j)i+1}\|_2}{\|\mathbf{A}_{|S^i}^{(j)} \mathbf{g}_k^{(j)i+1}\|_2}$, $k \in \{1, \dots, P\}, j \in \{1, \dots, N_{\text{rec}}\}$
 - 11: $i \leftarrow i + 1$
 - end while**
 - 12: return S^i
-

V. SIMULATION RESULTS

In this section, we compare the performance of our two algorithms, BSOMP and BSIHT, along with a simple union between the supports recovered by each receiver separately using SOMP. The union is performed by selecting the most common indices with respect to the receivers. In case of a tie, the indices are chosen uniformly at random so that the resulting

support contains κ entries. A success is declared whenever the recovered and original supports are exactly identical.

In the simulations, we consider a signal with Nyquist rate $f_{\text{Nyq}} = 6.1\text{GHz}$ composed of $N_{\text{sig}} = 3$ QPSK modulated transmissions with arbitrary carriers and single-sided bandwidth $B = 20\text{MHz}$. The transmissions are passed through Rayleigh channels with maximum shifting $2\sigma^2 = 500\text{MHz}$. Besides, we apply log-normal shadowing with the following parameters: reference distance $d_0 = 1$, path loss to the reference point $PL_0 = 0$, γ and X_σ are chosen arbitrarily from the sets of values $\{2.6, 2.4, 0, 3\}$, $\{14.1, 9.6, 0, 7\}$ respectively. These are common values describing different obstacles and propagation effects [26]. The distances between the transmitters and receivers are generated uniformly at random between 0 and 100.

For the sampling stage, we consider $N = 256$ spectral bands and $M = 15$ analog channels, each sampling at $f_s = 24\text{MHz}$ and with $N_s = 40$ samples per channel. The overall sampling rate of each receiver is thus 360MHz , which is a little below 6% of the Nyquist rate and 3 times the Landau rate. In all of the three algorithms, the sparsity is assumed to be known. Union and BSOMP use a sparsity-based halting criterion, whereas in BSIHT we fix the maximum iterations to be 10. Each experiment is repeated over 200 realisations.

We show the influence of several practical parameters on the performance of our recovery algorithms. In the first experiment, we illustrate the impact of SNR on the detection performance. Figure 1 shows the support recovery success rate of the three algorithms for different values of SNR

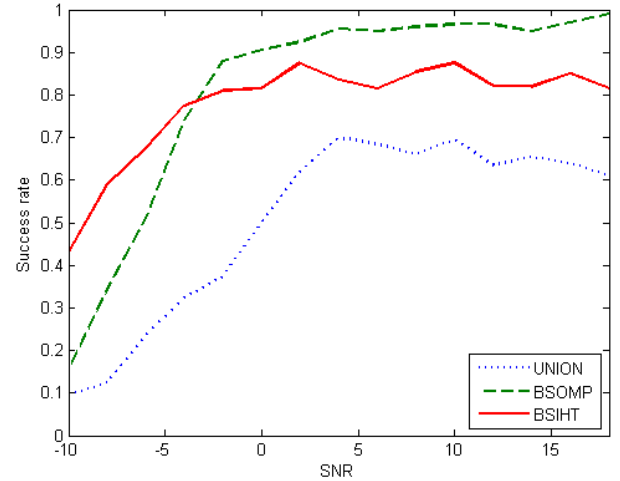


Fig. 1. Influence of the SNR on the success rate.

In the second experiment, we vary the sensing time. We consider the same sampling parameters as in the previous experiment and set the SNR to be 10dB. Figure 2 shows the support recovery success rate for different values of the number of samples.

In the third experiment, we vary the number of receivers N_{rec} . We consider the same parameters as above. Figure 3 shows the support recovery success rate for different values of the number of receivers. The jumps that occur for the union algorithm are due to the fact that in case of a tie, the fusion center has to choose arbitrarily between support indices with the same record. This considerably reduces the support

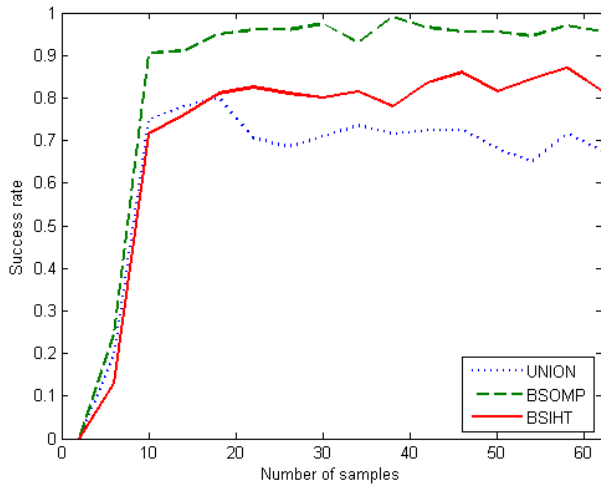


Fig. 2. Influence of the number of samples on the success rate.

detection performance for certain values of the number of CRs that favorise ties.

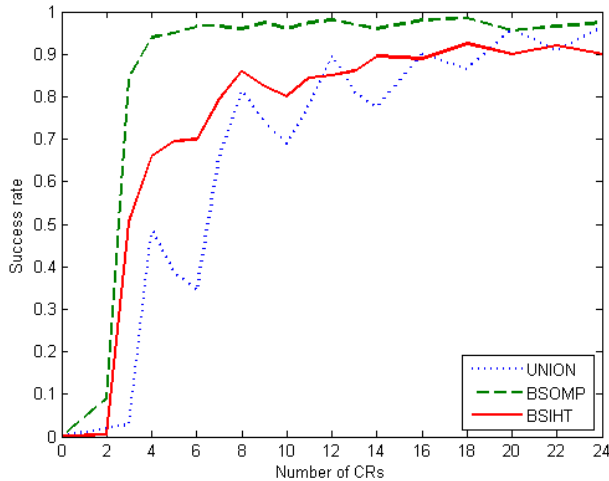


Fig. 3. Influence of the number of receivers CRs on the success rate.

VI. CONCLUSION

We have presented two soft decision based collaborative support recovery algorithms from sub-Nyquist samples: BSOMP and BSIHT. We use a real sampling scheme and do not assume that the CSI is known. We observe that BSOMP and BSIHT outperform a hard decision union algorithm for a large majority of parameters combination. Moreover, the success rate of BSOMP is generally higher than this of BSIHT.

REFERENCES

- [1] J. Mitola and C. Q. Maguire Jr., "Cognitive radio: Making software radios more personal," *IEEE Personal Commun.*, vol. 6, pp. 13–18, Aug. 1999.
- [2] S. Haykin, "Cognitive radio: Brain-empowered wireless communications," *IEEE J. Select. Areas Commun.*, vol. 23, pp. 201–220, Feb. 2005.
- [3] A. Ghasemi and E. S. Sousa, "Spectrum sensing in cognitive radio networks: requirements, challenges and design trade-offs," *IEEE Communications Magazine*, vol. 46, pp. 32–39, Apr. 2008.
- [4] E. G. Larsson and M. Skoglund, "Cognitive radio in a frequency-planned environment: Some basic limits," *IEEE Trans. Wireless Commun.*, vol. 7, pp. 4800–4806, Dec. 2008.
- [5] N. H. A. Sahai and R. Tandra, "Some fundamental limits on cognitive radio," *Proc. 42nd Annu. Allerton Conf. Commun., Control, and Computing*, pp. 1662–1671, Oct. 2004.
- [6] M. Mishali and Y. C. Eldar, "From theory to practice: Sub-Nyquist sampling of sparse wideband analog signals," *IEEE J. Sel. Topics Signal Process.*, vol. 4, no. 2, pp. 375–391, Apr. 2010.
- [7] —, "Blind multi-band signal reconstruction: Compressed sensing for analog signals," *IEEE Trans. on Signal Process.*, vol. 57, no. 3, pp. 993–1009, Mar. 2009.
- [8] D. D. Ariananda and G. Leus, "Compressive wideband power spectrum estimation," *IEEE Trans. on Signal Process.*, vol. 60, pp. 4775–4789, Sept. 2012.
- [9] M. A. Lexa, M. E. Davies, J. S. Thompson, and J. Nikolic, "Compressive power spectral density estimation," *IEEE ICASSP*, 2011.
- [10] D. Cohen and Y. C. Eldar, "Sub-nyquist sampling for power spectrum sensing in cognitive radios: A unified approach," *IEEE Trans. on Signal Process.*, vol. 62, pp. 3897–3910, Aug. 2014.
- [11] I. F. Akyildiz, B. F. Lo, and R. Balakrishnan, "Cooperative spectrum sensing in cognitive radio networks: A survey," *Phys. Commun.*, vol. 4, pp. 40–62, Mar. 2011.
- [12] A. Ghasemi and E. S. Sousa, "Collaborative spectrum sensing for opportunistic access in fading environments," *IEEE Int. Symp. New Frontiers in Dynamic Spectrum Access Networks (DySPAN)*, pp. 131–136, Nov. 2005.
- [13] F. Y. Suratman, A. Tetz, and A. M. Zoubir, "Collaborative spectrum sensing using sequential detections: soft vs. hard decision," *Int. Conf. of Information and Commun. Technology (ICOICT)*, pp. 1–6, Mar. 2013.
- [14] Z. Quan, S. Cui, A. H. Sayed, and H. V. Poor, "Optimal multiband joint detection for spectrum sensing in cognitive radio networks," *IEEE Trans. on Signal Process.*, vol. 57, pp. 1128–1140, 2009.
- [15] J. Meng, W. Yin, H. Li, E. Hossain, and Z. Han, "Collaborative spectrum sensing from sparse observations in cognitive radio networks," *IEEE J. Sel. A. Commun.*, vol. 29, pp. 327–337, Feb. 2011.
- [16] D. D. Ariananda and G. Leus, "Cooperative compressive wideband power spectrum sensing," *IEEE Asilomar Conf. on Signals, Systems, and Computers*, pp. 303–307, Nov. 2012.
- [17] A. Makhzani and S. Valaee, "Reconstruction of jointly sparse signals using iterative hard thresholding," *IEEE Int. Conf. on Commun. (ICC)*, pp. 3564–3568, 2012.
- [18] J. A. Bazerque and G. B. Giannakis, "Distributed spectrum sensing for cognitive radio networks by exploiting sparsity," *IEEE Trans. on Signal Process.*, vol. 58, pp. 1847–1862, Mar. 2010.
- [19] M. F. Duarte, S. Sarvotham, D. Baron, M. B. Wakin, and R. G. Baraniuk, "Distributed compressed sensing of jointly sparse signals," *IEEE Asilomar Conf. Signals, Systems, and Computers*, pp. 1537–1541, 2005.
- [20] S. M. Mishra, A. Sahai, and R. W. Brodersen, "Cooperative sensing among cognitive radios," *IEEE Int. Conf. on Commun. (ICC)*, pp. 1658–1663, 2006.
- [21] B. Sklar, "Rayleigh fading channels in mobile digital communication systems part I: Characterization," *IEEE Commun. Magazine*, vol. 35, pp. 90–100, Jul. 1997.
- [22] V. Erceg, L. J. Greenstein, S. Y. Tjandra, S. R. Parkoff, A. Gupta, B. Kulic, A. A. Julius, and R. Bianchi, "An empirically based path loss model for wireless channels in suburban environments," *IEEE J. Sel. Areas Commun.*, vol. 17, pp. 1205–1211, Sep. 2006.
- [23] R. Venkataramani and Y. Bresler, "Perfect reconstruction formulas and bounds on aliasing error in sub-Nyquist nonuniform sampling of multiband signals," *IEEE Trans. Inf. Theory*, vol. 46, pp. 2173 – 2183, Sept. 2000.
- [24] J. Tropp, A. C. Gilbert, and M. J. Strauss, "Simultaneous sparse approximation via greedy pursuit," *IEEE ICASSP*, vol. 5, pp. 721–724, Mar. 2005.
- [25] Y. C. Eldar, P. Kuppinger, and H. Bölcskei, "Block-sparse signals: Uncertainty relations and efficient recovery," *IEEE Trans. on Signal Process.*, vol. 58, pp. 3042–3054, Jun. 2010.
- [26] T. S. Rappaport, *Wireless communications principles and practices*. Prentice Hall, 2002.